STRUCTURAL AND MAGNETIC STUDIES OF COBALT SUBSTITUTED NICKEL ZINC FERRITES

VENKATA KUMAR VAGOLU, K. SAMATHA,
DEPARTMENT OF PHYSICS, ANDHRA UNIVERSITY, VISAKHAPATNAM – 530 003. ANDHRA PRADESH, INDIA, venkatvagolu@gmail.com; samathak2002@yahoo.com

K. CHANDRA MOULI,
DEPARTMENT OF ENGINEERING PHYSICS, A. U. COLLEGE OF ENGINEERING, ANDHRA UNIVERSITY, VISAKHAPATNAM – 530 003. ANDHRA PRADESH, INDIA, ckemburu@yahoo.com

J. N. KIRAN,
DEPARTMENT OF ENGINEERING PHYSICS, VIGNAN UNIVERSITY, VADLAMUDI, GUNTUR DIST. ANDHRA PRADESH, INDIA,kiran.nichal@gmail.com

D. SANTHI PRIYA AND PAUL DOUGLAS SANASI *
DEPARTMENT OF ENGINEERING CHEMISTRY, A. U. COLLEGE OF ENGINEERING, ANDHRA UNIVERSITY, VISAKHAPATNAM – 530 003. ANDHRA PRADESH, INDIA, santhipriya78@yahoo.com; pauldouglas12@gmail.com

ABSTRACT:

Cobalt substituted Nickel-zinc ferrites of different compositions $Ni_{0.95-x}Zn_{0.05}Co_xFe_2O_4$ and $Zn_{0.95-x}Ni_{0.05}Co_xFe_2O_4$ (where x = 0.00, 0.01, 0.02,0.03, 0.04, 0.05 and 0.06).have been prepared by citrate precursor method involving concerned metals and mixing them in solution state. Parts of the sol-gel powder heated at elevated temperatures were characterized by X-ray diffraction (XRD), Particle size analyser and Scanning Electron Microscope (SEM) to reveal the crystallized single phase structure of the ferrite. In addition to that magnetic properties were measured. The initial magnetic permeability was found to increase with the increasing of the frequency as a result of the domain wall motion and the corresponding loss was small.

KEYWORDS: COBALT SUBSTITUTED NICKEL-ZINC FERRITES; CITRATE-PRECURSOR METHOD; STRUCTURAL CHARACTERISATION, MAGNETIC PROPERTIES

INTRODUCTION

Co substituted Ni–Zn ferrites are widely used in wave absorbers to suppress the electromagnetic interference among devices up to microwave frequencies [1], high frequency switching magnets and magnetic pulse compressors [2, 3], antenna rods for radios [4], transformers, reactor cores, etc. Ni–Co–Zn ferrite exhibits enhanced magnetic properties and hence they are useful as ferromagnetic core materials. Polycrystalline ferrites have been extensively used in many electronic devices, because of their high electrical resistivity, mechanical hardness and chemical stability.

EXPERIMENTAL PROCEDURE

Synthesis:

The nano ferrites have been synthesised by soft chemical routes. For chemical synthesis, a precursor compound with an intended stoichiometry is first prepared and is decomposed at temperatures (<873 K) in a subsequent calcination reaction to obtain the required metal oxides [5]. The citrate precursors are usually preferred due to their low solubility, low decomposition temperature and very fine particle nature [6]. Ideally, in order to achieve a complete reaction within the shortest time and at the lowest possible temperatures, mixing of the component cations on an atomic scale is necessary. Compound precursors achieve this goal, but the stoichiometry of the precursors does not often strictly coincide with the stoichiometry of the desired product [7]. Various authors [8, 9] have investigated co-precipitation of metal citrates from appropriately composed solutions in order to produce precursor compounds for spinel ferrites MFe_2O_4. Wickham [10] has synthesized spinel ferrites MFe_2O_4 (where M = Mg^{2+}, $Ni^{2+,}$ $Zn^{2+,}$ Mn^{2+} or CO^{2+}) in air at 873 K.

Sample Preparation:

A series of ferrites with composition $Ni_{0.95-x}Zn_{0.05}Co_xFe_2O_4$ were chosen for this study. All the reagents used were of AR grade. Aqueous solution of stoichiometric amounts of Nickel, zinc, Cobalt nitrates and ferric citrate were reacted with citric acid in 1:1 molar ratio. pH of the solution was increased to 7 by addition of ammonium hydroxide to complete the reaction. Ethylene glycol was added to the mixture and the solution was evaporated very slowly over a period of ten to twelve hours to dryness. Viscosity and color changed as the sol

turned into puffy, porous dry gel. As soon as the solvent removal is completed, dried precursor undergoes a self-ignition reaction to form a very fine powder known as as-synthesized powder. The as-synthesized powder thus obtained was treated in a furnace at 800^0C for 2 hours to remove the residual carbon. A number of pellets were prepared by weighing a known amount of the powder by pressing them into pellets of 12mm diameter and a thickness of 2mm for further studies and sintered at 900-1200^0C for two hours in air.

The XRD spectra were recorded on PANalytical-Xpertpro diffractometer. The microstructural were studied with a Scanning Electron Microscope (SEM) model JEOL –JSM 6610 LV. FTIR spectra were recorded on BRUKER ALPHA FTIR with Opus 6.1 version. Magnetization M(H) measurements were made using a commercial vibrating sample mag- netometer (VSM) model BHV-50 of Riken Denshi Co. Ltd. Japan. The DC resistivity measurement were carried out by 2 probe method. The dielectric measurements were made by LCR-Q model HP-4284A in the frequency range 20Hz to 10M HZ for toroidal samples.

RESULTS AND DISCUSSION

A. Characterisation:

FT-IR:

In order to confirm the formation of the spinel phase and to understand the nature of the residual carbon in the samples, the FTIR spectra of the as-synthesized powders and thermally treated powder were recorded, Figure (1). The as-synthesized sample shows characteristic absorptions of ferrite phase with a strong absorption around 600 cm^{-1} and weak absorption in the range 410-450 cm^{-1}[8]. This difference in the band position is expected because of the difference in the Co^{2+} distance for the octahedral and tetrahedral compounds. Waldron [10] studied the vibrational spectra of ferrites and attributed the sharp absorption band around 600 cm^{-1} to the intrinsic vibrations of the tetrahedral groups and the other band of the octahedral groups.

There are two weak and broad absorptions around 1400 and 1600 cm^{-1} corresponding to the presence of small amount of residual carbon in the samples. These absorptions in the present case are very weak which indicate that the residual carbon has mostly burnt away during the sintering process.

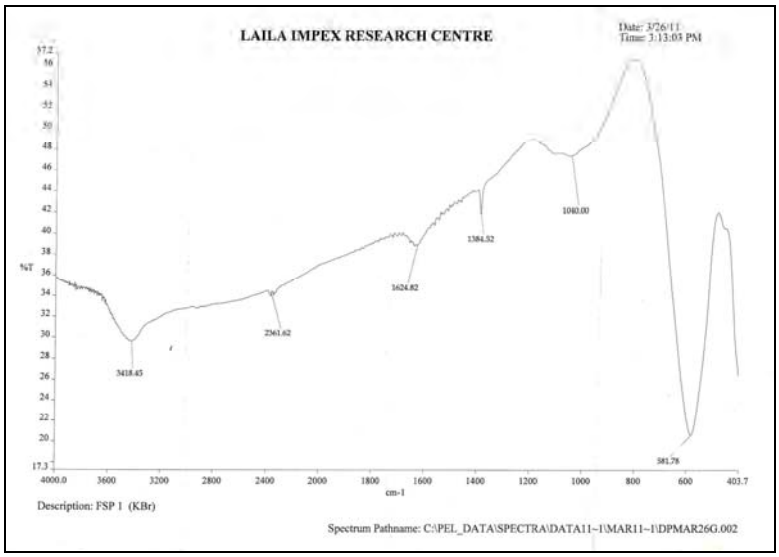

Fig.1 : Typical FTIR spectra of cobalt substituted Nickel zinc ferrite

X-Ray Diffractograms (XRD)

Figure (2) shows a typical XRD pattern for samples sintered at 800^0 C. The pattern shows all the characteristic peaks of a spinel structure and confirms the phase formation indicating the absence of other impurity phases. All the peaks perfectly match with the crystalline phase of cubic spinel structure of Ni-Zn ferrite (JCPD Card No. 008-0234).The lattice parameters were calculated using XRD data and it is observed that there is a compositional variation in lattice parameter. The lattice parameter for all the Co-substituted Ni– Zn ferrites increase with increasing Co content, which can be attributed to the larger ionic radius of Co^{2+} (0.78 A°) than Ni^{2+} (0.74 A°). The linear variation of the lattice parameter with respect to Co concentration fulfills the condition of Vegard's law. From the data on average crystallite size of sintered powder determined by x-ray diffraction using the Debye–Scherer formula for the Co-substituted Ni–Zn ferrites, it is seen that the average crystallite size for the sintered powder of different compositions of Ni–Co–Zn ferrites is found to be in the range of 25–28 nm. The values of crystallite size evaluated from XRD (FWHM) are in agreement with those reported by Parvatheeswara Rao et al [11].

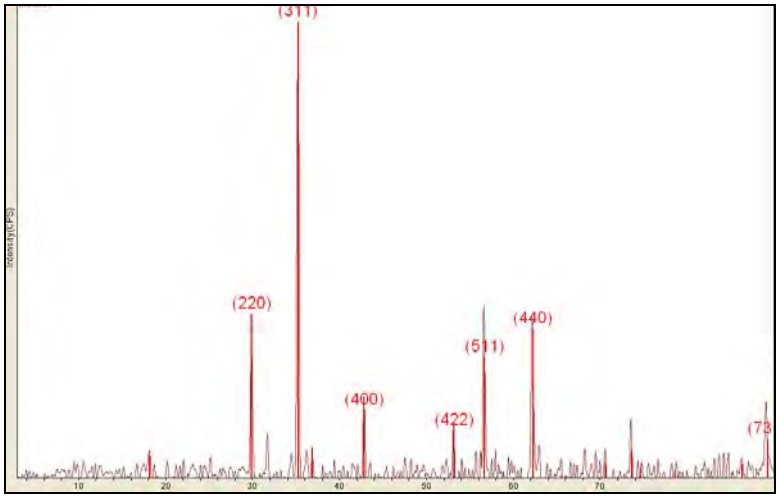

Figure 2- Typical XRD Spectral Patterns of the cobalt substituted Nickel zinc ferrite

Surface Morphology(SEM)

Figure 3 shows the typical SEM micrographs sintered at 800◦C. The average grain size was calculated by the line intercept method. It is observed that the average grain size decreases with the addition of cobalt, as tabulated in table 3. It is seen that, as x increases, the grain size decreases appreciably.

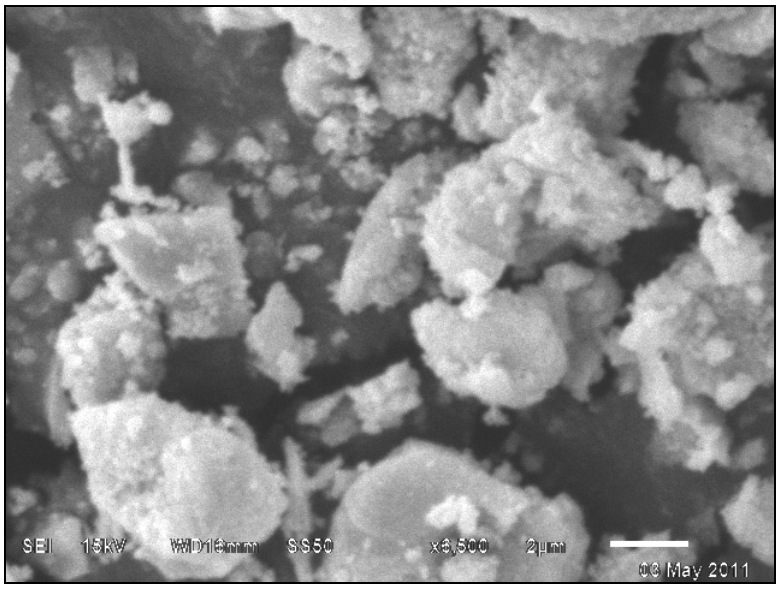

Figure 3: Typical Surface Morphology of cobalt substituted Nickel Zinc Ferrites

Effect of cobalt substitution on the magnetic properties of Ni-Zn ferrites:

Cobalt substituted Nickel Zinc ferrite samples having the chemical formula $Ni_{0.95-x}Zn_{0.05}Co_xFe_2O_4$ (NZCF) and $Zn_{0.95-x}Ni_{0.05}Co_xFe_2O_4$ (ZNCF) (where x = 0.00, 0.01, 0.02,0.03, 0.04, 0.05 and 0.06). The present samples belong to cubic system of ferromagnetic spinals. In these systems the magnetic order is mainly due to an upper exchange interaction mechanism occurring between the metal ions in the 'A' and 'B' sub lattices. The substitution of Co^{2+} ions, which has a preferential 'A' site occupancy results in the reduction of the exchange interaction between 'A' and 'B' sites. Hence magnetic properties of the fine particles can be varied by varying the degree of cobalt substitution.

Room temperature magnetic parameters measurements of ZNCF and NZCF fine particles:

Magnetic parameters, namely the specific magnetization (M_s), remnant magnetization (M_r) and coercive field (H_c) of the prepared fine particles ZNCF and NZCF were measured at room temperature in a maximum field of 10 KG (10000 gauss) .Magnetic properties of ZNCF and NZCF are strongly dependent on the cobalt concentration . The room temperature magnetization curves of ZNCF and NZCF are given in Fig. 4 and Fig 5. These show the variation of magnetization, coercive field with cobalt content.

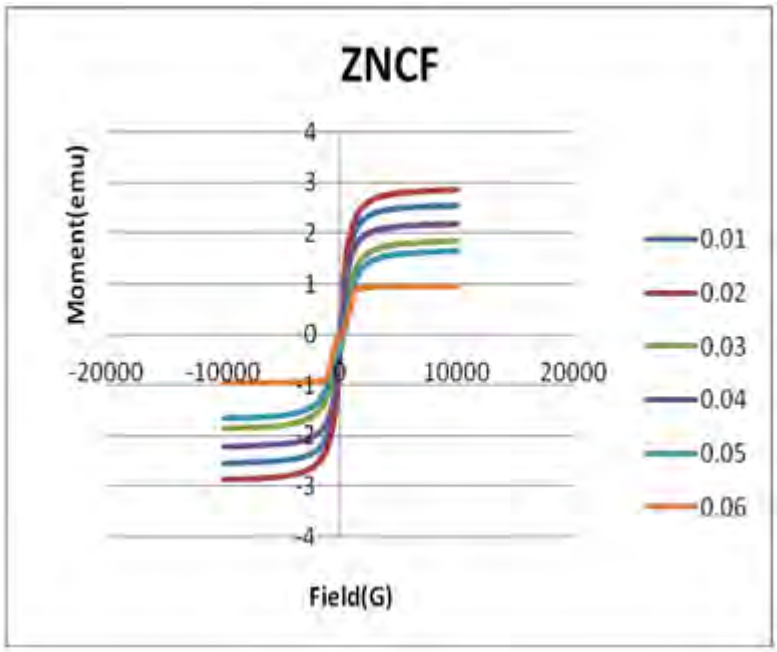

Figure 4 Magnetization curves for ZNCF

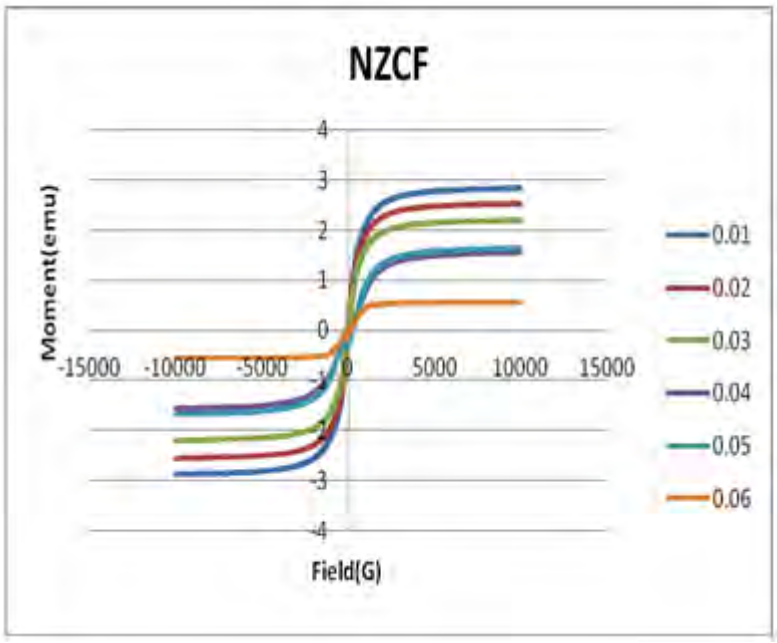

Figure 5 Magnetization curves for NZCF

The saturation magnetization (Ms) for ZNCF was found to decrease from x= 0.01 to x=0.03, here is an increase in Ms for x= 0.04 and it is very low for x= 0.05 and x= 0.06 respectively. The Ms for NZCF sample was found to increase from x= 0.01 to x= 0.02 (upon cobalt substitution) .for x= 0.03, Ms is very low. It is observed that the saturation magnetization decreases from x= 0.04 to x=0.06. The respective reduction in magnetization can be due to a rearrangement of cations because of the changed preferential occupancy in the case of nanosized ferrites i.e., a change in distribution of Ni 2+ and Zn 2+ on the two sites.

The saturation magnetization of samples decreases with decrease in cobalt concentration ZNCF (x=0.06 to x= 0.03) and NZCF (x=0.06 to x=0.03). This may be due to the relatively high orbital contribution of Co^{2+} ions to the magnetic moment, which gives large induced anisotropy. In ferrites two magnetic ions are separated by nonmagnetic ion (in this case Oxygen). Hence magnetic ions have a magnetic interaction mediated by the electrons in their common nano magnetic neighbors, which is more important than their direct exchange interactions referred to as super exchange interaction. The presence of ions in the form of impurity (or) an absence of the oxygen ions at the surface leads to breakage of super exchange bonds between magnetic cations, including a large surface spin disorder (12). However, the low values of saturation magnetization obtained in the

present work suggest that the mixed spinal structure is not likely to be present in our case. This plays an active role in the decline of magnetization values (13,14). With the increasing cobalt incorporation the coercivity is showing a continuous increase, shown in Fig.4 and Fig.5 respectively for ZNCF and NZCF, this is attributed to the fact that coercive field (Hc) is directly proportional to the magneto crystalline anisotropy constant. A small number of Co^{2+} ions enter in to the spinal lattice, leading to the appearance of the spin-orbital coupling which determines the magnetic anisotropy in the ferrites. Therefore as the cobalt content increases, the magneto crystalline anisotropy increases, this decreases the domain wall energy resulting in high coercive force. Reduction in the coercive field Mr for ZNCF(x=0.05) and NZCF (x=0.06) samples may be due to partial substitution of Co^{2+} ion, due to size effect or due to the presence of super paramagnetic particles.

Another important factor which influences the magnetization of ferrites is the microstructure. The individual grain acts as magnetic dipole having certain amount of saturation magnetization. These grains form a magnetic circuit to produce resultant saturation magnetization. The presence of pores breaks the magnetic circuits present among the grains and results in a net reduction of magnetic properties with increasing pore concentration (15). In this present report, the average grain size of the ferrite phase goes on increasing with cobalt content and results in a decrease in porosity; as a result saturation magnetization increases.

3.3. Compositional variation of initial permeability (μ_i)

Figure 6 shows compositional variation of initial permeability measured at 1 kHz for the ferrite system NZCF and ZNCF. It is observed that the initial permeability decreases with increasing cobalt content. The decreasing trend in μ_i can be attributed to the domain wall energy, magnetocrystalline anisotropy constant (K_1) and magnetostriction constant (λ_s). Kulikowski et al [20] have observed with increasing cobalt content the domain wall energy increases and the value of initial permeability (μ_i) decreases. There would also be expected a monotonic increase in λ value. The contribution of cobalt ions to the magnetostriction of Ni–Zn ferrite has the same origin as the magneto crystalline anisotropy constant. The magnetostrictive effect is connected with cobalt ions which occupies octahedral sites of the spinal. Similar observations are observed in our case also. The values of (K_1) are calculated by taking the end values of the corresponding ferrites and taking into consideration the stoichiometry of the composition. The initial permeability μ_i decreases for a mixed Ni–Zn ferrite. This decrease in initial permeability μ_i may be due to the cobalt ion having positive magneto crystalline anisotropy K_1 and the addition of Co^{2+} in a small quantity is expected to increase μ_i through compensation of the negative K_1 of excess Ni–Zn ferrite. However, the proportion of Co^{2+} selected appears to cross the zero K_1 range and hence the μ_i shows a reverse trend. Therefore, a marginal contribution to μ_i may also come from D (grain size) which tends to decrease. Saturation magnetization Ms, however, does not show significant variation. On a bulk level the higher density will lead to high μ_i but there is no significant change in density to modulate μ_i significantly. Thus a decrease in μ_i is attributable to an increase in K_1.

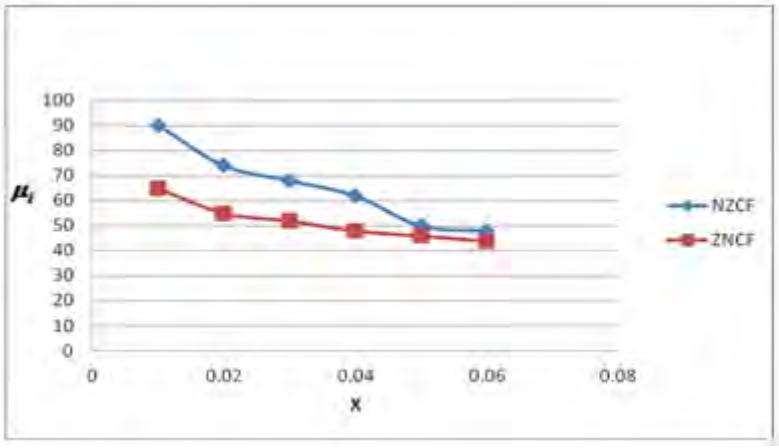

Figure 6Compositional variation of initial permeability (μ_i) measured at 10 kHz.

3.4. Thermal variation of initial permeability (μ_i)

Figures 7,8 and 9 show the initial permeability (μ_i), its real part (μ'_i), and imaginary part (μ_i'') vary with temperature for the composition NZCF and ZNCF systems in the range from room temperature to the Curie temperature (T_c). Near T_c both μi and μ_i' drop to zero sharply. A sharp decrease in μ_i and μ_i'suggests single-phase formation of the ferrite material. This observation supports the conclusion drawn from the XRD analysis that all the compositions are single phase. In most of the magnetic materials, μ_i increase with temperature up to the Curie temperature T_c. This is because the anisotropy field usually decreases faster with temperature than Ms [26]. Both Enz [27] and Ohta [28] have shown that the initial permeability (μ_i) is maximum at the temperature

where the anisotropy constant K_1 changes sign. From the thermal variation of (μ_i'', it is seen that with the increase of temperature (μ_i''increases, reaches a maximum near T_c and then falls sharply near to T_c. The loss becomes large near T_c, which may be due to the damping effect of the domain walls which may be very small. From thermal variation of the initial permeability for the composition NZCF and ZNCF systems with x = 0.00, 0.01, 0.02, 0.03, 0.04, 0.05 and 0.06, peaking behaviour is observed at T_c. The Hopkinson peak indicates the presence of SD grains. Hence it can be concluded that there is dominance of SD grains.

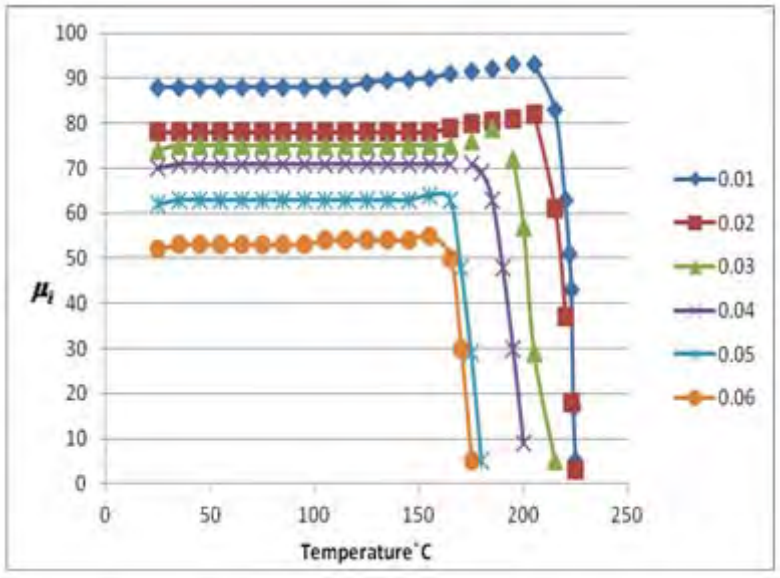

Figure 7 Thermal variation of initial permeability (μ_i) for ferrite system NZCF

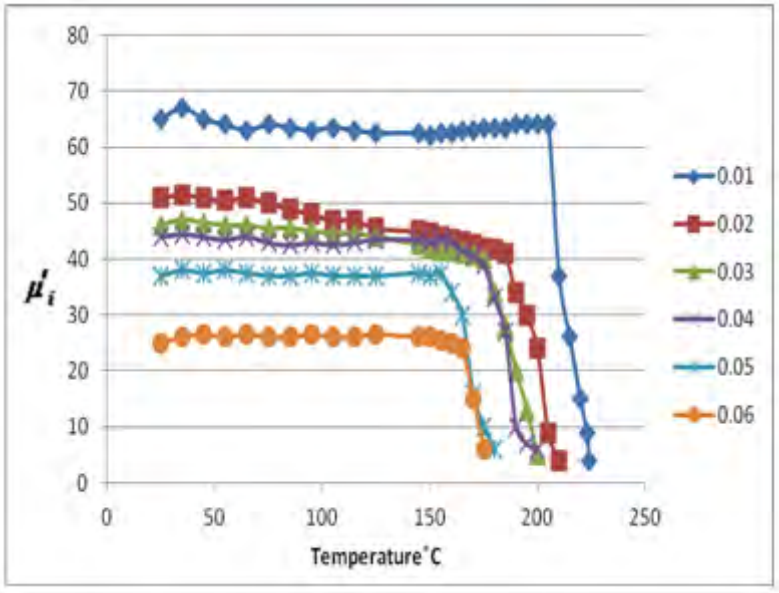

Figure 8 Thermal variation of initial permeability (μ_i') for ZNCF system.

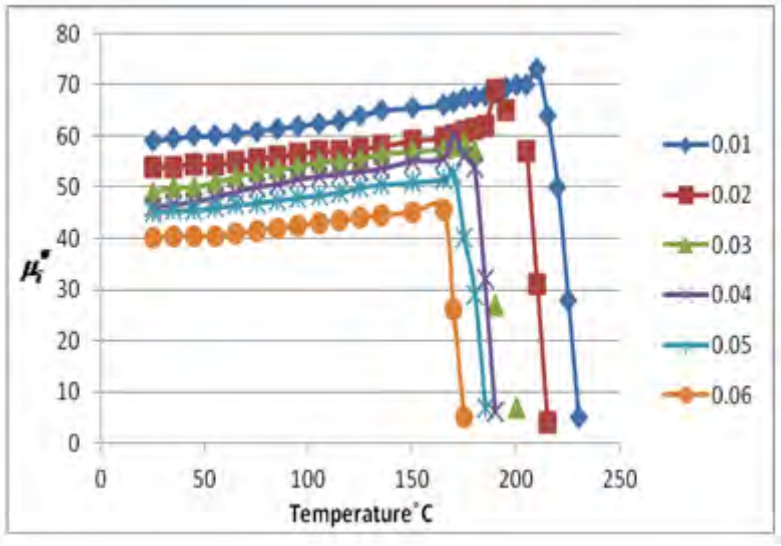

Figure 9 Thermal variation of initial permeability (μ_i') for NZCF system

3.5. Frequency dependence of initial permeability (μ_i)

In figures 10 and 11 variation of $\mu_i'$and ($\mu_i''$with frequency in the range 20 Hz–10 MHz, for the composition NZCF and ZNCF , are shown. Rado [29] and others [30–33] observed high frequency dispersion and absorption in μi and attributed it to rotational resonance in the combined anisotropy and demagnetizing fields while the low frequency dispersion was attributed to the domain wall displacement. From figures 7 and 8 frequency variation of $\mu_i'$and μ_i'' clearly indicate the low frequency dispersion which may be attributed to the domain wall movement. We have already shown that the major contribution to μ_i is due to domain wall displacement, which is manifested here by the low frequency dispersion. The dispersion at high frequencies (=1 MHz) is attributed to spin resonance in the internal anisotropy field.

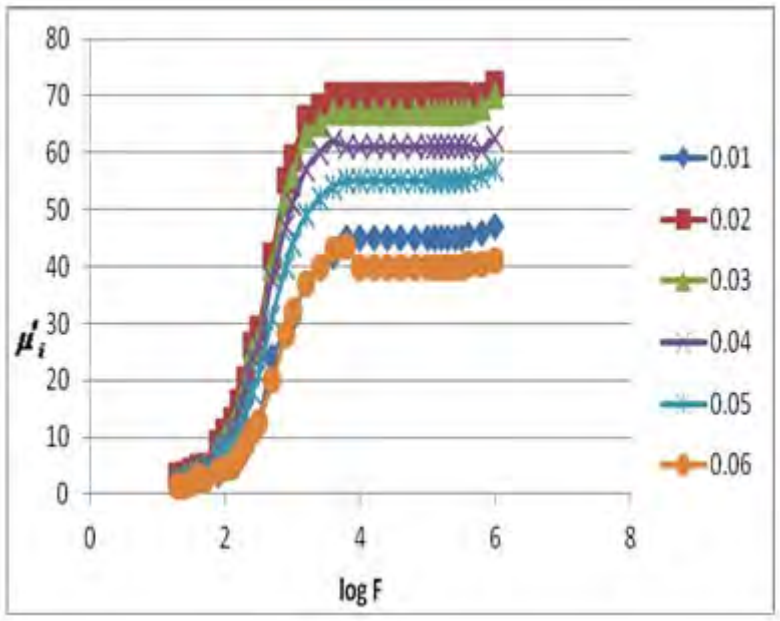

Figure 10 Frequency variation of initial permeability (μ_i')

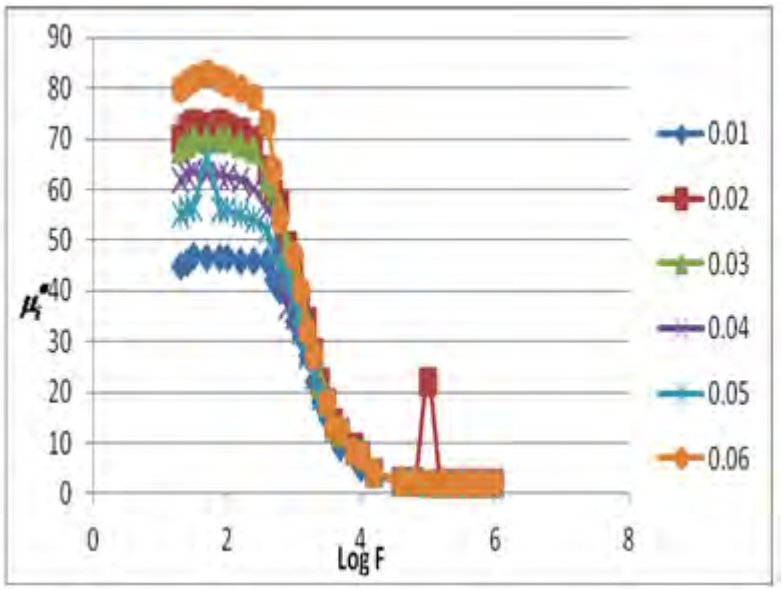

Figure 11 Frequency variation of initial permeability (μ_i'')

3.6. Loss factor (LF)

The ratio of the imaginary part of the permeability representing the losses in the material to the real part of the permeability is a measure of the inefficiency of the magnetic system. It is called the loss tangent: Loss tangent = tan $\delta = \mu_i'/\mu_i''$, the loss factor is defined as LF = tan δ/μ_i. This loss factor (LF) parameter should be as low as possible.

In figure 12 dispersions of LF for the composition NZCF and ZNCF are shown. With the increase of frequency from 20 to 200 Hz, the LF decreases. In most of the compositions the LF value is almost constant in the frequency range 10–100 kHz. In figure 13 thermal variation of the loss factor for the composition NZCF and ZNCF is shown. In the temperature range 25^0 C to near T_c, it is found that LF is almost constant, while above T_c the loss factor increases exponentially. The thermal variation of tan δ seems to be responsible for the increase in loss factor. In order to have a low loss factor the ferrite must be operated below the Curie temperature. And it is observed that the loss factor parameter for both the NZCF and ZNCF is following similar trend.

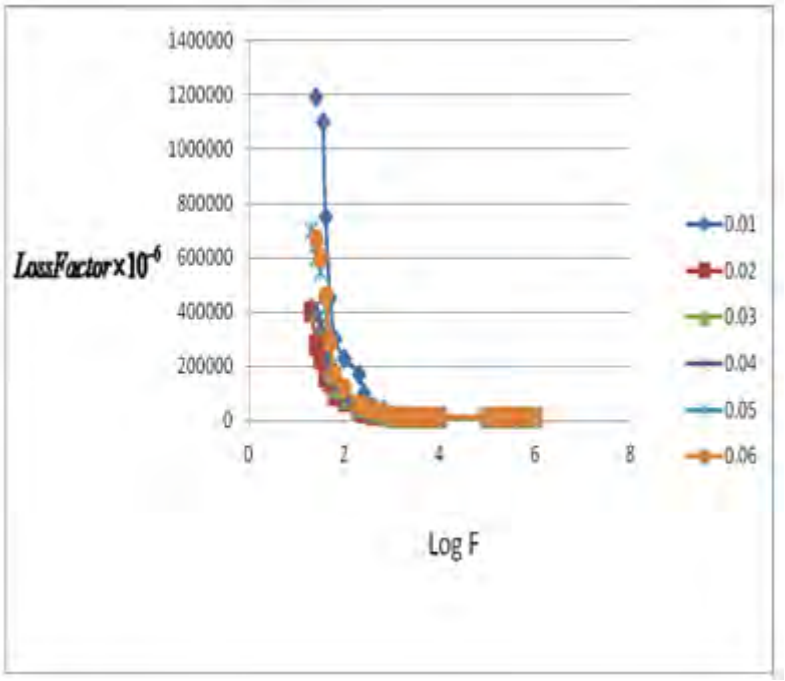

Figure 12 Frequency variation of loss factor (LF)

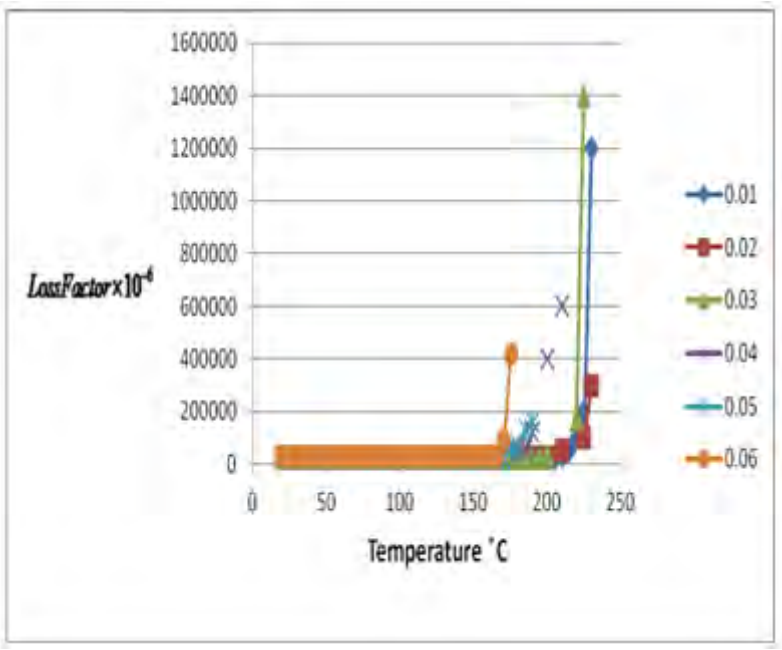

Figure 13 Thermal variation of loss factor for ferrite system

CONCLUSION

Samples of Nanocrystalline Cobalt substituted Ni–Zn ferrites have been successfully prepared by employing the co-precipitation technique using citrate precursors. The x-ray diffraction confirms the phase formation of the sintered ferrite. It is further observed that the lattice parameter a (°A) increases with the addition of Co^{2+} ions in the Ni–Zn ferrite matrix. From the the permeability measurements, it is observed that with increasing cobalt content, the domain wall energy increases and the value of initial permeability µi decreases. The values of saturation magnetization Ms and nB of all compositions are almost independent of cobalt content.

References

[1] Kang D H, Shin J Y and Oh J H 1992 Proc. 6th Int. Conf. on Ferrites (Tokyo and Kyoto, Japan)
[2] Shinde R S, Bhasin H K and Karmarkar M G 1997 7th Int.Conf. on Ferrites (Bordeaux, France); J. Phys. IV France 7 C1-149–50
[3] Shinde R S, Pareek P and Yadav R R 2004 Proc. APAC (Gyeongju, Korea) p 699
[4] Bradley F N 1971 Materials for Magnetic Functions (New York: Hayden)
[5] Bremer M, Fisher S, Topelmann H and Scheler H 1992 Thermochim. Acta 209 323
[6] Paulus M 1972 Preparative Methods in Solid State Chemistry ed O Hagenmuller (New York: Academic) p 487
[7] Longo J M, Horowitz H S, Clevenna L R, Holt S L, Milstein J L and Robbins M (ed) 1986 Solid State Chemistry—A Contemporary Overview (Advances in Chemistry Series) (Washington, DC: American Chemical Society) p 139
[8] SchueleW J 1959 J. Phys. Chem. 63 83
[9] Klienert P and Funke A 1961 J. Chem. 1/5 155
[10] R.D. Waldron, Phys. Rev. 99(1955)1727.
[11] Parvatheeswara Rao B, Mahesh Kumar A, Rao K H, Murthy Y L N, Caltun O F, Dumitru I and Spinu L 2006 J. Optoelectron. Adv. Mater. 8 1703
[12] Sankpal A M, Kakatkar S V, Choudhari N D, Patil R S, Sawant S R and Suryavanshi S S 1998 J. Mater. Sci. Mater. Electron. 9 173
[13] J M D Coey, Phys Rev. Lett., 27, (1971), 1140
[14] M Garcia del Muro, X BatIle and A Labarta, Phys. Rev.: B 59, (1999) ,13584
[15] Rao B P, Subba Rao P S V and Rao K H 1996 J. Mater. Sci. 15 781
[16] Kulikowski J and Bienkowski A 1982 J. Magn. Magn. Mater.26 297
[17] Rezlescu N, Rezlescu E, Popa P D, Craus M L and Rezlescu L 1998 J. Magn. Magn. Mater. 182 199
[18] Enz U 1961 Proc. Inst. Electron. Eng. 109B 246
[19] Ohta K 1963 J. Phys. Soc. Japan 18 685
[20] Rado G T 1953 Rev. Mod. Phys. 25 81
[21] Rado G T, Floen V J and EmersonW H 1957 Proc. Inst.Electron. Eng. B 1045 198
[22] Rado G T and Terries A 1952 Phys. Rev. 88 909
[23] Rado G T, Wright R W and EmersonW H 1950 Phys. Rev. 80 273
[24] Sankpal A M, Kakatkar S V, Choudhari N D, Patil R S,Sawant S R and Suryavanshi S S 1998 J. Mater. Sci. Mater.Electron. 9 173